

## Nonuniform segregation of Ga at AlAs/GaAs heterointerfaces

Wolfgang Braun,\* Achim Trampert, Lutz Däweritz, and Klaus H. Ploog  
*Paul-Drude-Institut für Festkörperelektronik, Hausvogteiplatz 5-7, D-10117 Berlin, Germany*  
 (Received 5 August 1996)

Segregation at GaAs/AlAs (001) heterointerfaces has been studied experimentally by an *in situ* electron diffraction technique during molecular-beam epitaxy and by *ex situ* transmission electron microscopy. Whereas the GaAs-on-AlAs interface is abrupt, we find Ga segregating up to 20 crystal planes when depositing AlAs on GaAs(001). The measurements indicate an anisotropic in-plane structure of this interface with elongated  $\text{Al}_x\text{Ga}_{1-x}\text{As}$  regions extending along  $[\bar{1}10]$ . Our findings provide insight into both the segregation mechanism and electron diffraction from growing surfaces at glancing angles. [S0163-1829(97)04004-6]

### I. INTRODUCTION

Semiconductor heterojunctions composed of the closely lattice-matched constituents GaAs and  $\text{Al}_x\text{Ga}_{1-x}\text{As}$  are considered as prototype heterointerfaces in terms of abruptness and structural perfection of the interface as well as regarding their potential for electronic band-gap engineering in advanced devices.<sup>1</sup> However, the perfection of such heterostructures is limited by fundamental physical effects, particularly by surface segregation phenomena.<sup>2-8</sup> The Ga segregation in the AlAs-GaAs(001) materials system, leading to pronounced asymmetries between the normal (AlAs deposited on GaAs) and inverted (GaAs on AlAs) interfaces, serves as a case study in this field.<sup>9-14</sup>

The broadening of the interface during its formation at moderate temperatures is generally described by thermodynamical models based on the difference of the bulk and surface chemical potentials.<sup>15</sup> At lower temperatures, the exchange process becomes kinetically limited, and models have been proposed that involve a step-mediated process.<sup>16</sup> At higher growth temperatures, the segregating species can desorb from the surface, leading to a steeper compositional slope. At still higher temperatures, bulk diffusion again broadens the interface.<sup>17</sup> In this paper, we concentrate on the thermodynamical equilibrium range where both low-temperature kinetical limitations and desorption/diffusion can be neglected. For GaAs/AlAs(001), this temperature range is approximately 500–610 °C, where most heterostructures are grown.<sup>9</sup> We show that Ga segregates many lattice planes into the overgrowing AlAs(001). In addition, this Ga segregation exhibits a strongly anisotropic in-plane structure, which we directly monitor by reconstruction-induced phase shifts (RIPS) of reflection high-energy electron diffraction (RHEED) intensity oscillations during molecular-beam epitaxy (MBE) growth of the interfaces. No measurable segregation is found at the (inverted) GaAs-on-AlAs (001) interface. These results are confirmed by high-resolution transmission electron microscopy (HRTEM) along  $[110]$  and  $[\bar{1}10]$ . The existence of a distinct lateral structure and the dependence of segregation on growth rate and sample temperature demonstrate the need for the three-dimensional treatment of the segregation problem. In addition, our findings reveal a new understanding of RHEED intensity oscillations and demonstrate the general applicabil-

ity of this method to monitor the formation of heterointerface in real time on an atomic scale.

### II. EXPERIMENT

In our experiments, GaAs and  $\text{Al}_x\text{Ga}_{1-x}\text{As}$  were deposited by MBE on GaAs(001) substrates using elemental sources in a continuous series of 30-s growth pulses separated by 30-s growth interruptions. The deposition rate was typically 0.2 nm/s. The 20-keV electron beam impinged at angles ranging from 0.2° to 1.5° along a high-symmetry azimuth and the resulting intensity oscillations were recorded at different positions of the diffraction pattern. Throughout the growth sequence, the diffraction conditions were kept constant. This procedure eliminated diffraction-related effects such as the dependence of the oscillation phase on electron beam incidence angle.<sup>18,19</sup> The growth sequence was designed to contain both homoepitaxial and heteroepitaxial pulse successions so that all four possibilities, GaAs on GaAs,  $\text{Al}_x\text{Ga}_{1-x}\text{As}$  on GaAs,  $\text{Al}_x\text{Ga}_{1-x}\text{As}$  on  $\text{Al}_x\text{Ga}_{1-x}\text{As}$ , and GaAs on  $\text{Al}_x\text{Ga}_{1-x}\text{As}$ , were present. The curves were then superimposed with respect to the onset of growth by means of the shutter actuation signal.

### III. RESULTS AND DISCUSSION

A comparison of both heteroepitaxial and homoepitaxial RHEED intensity traces for GaAs and AlAs is shown in Fig. 1. AlAs growth on GaAs is compared to AlAs growth on AlAs and GaAs growth on AlAs is compared to GaAs growth on GaAs. The oscillations from the heterointerface formation are found to be shifted with respect to the homoepitaxial reference oscillations. This phase shift is opposite in direction, but of equal magnitude for normal and inverted heterointerfaces. It has the same final value for the specular spot and the  $\{01\}$  reflections. The transition distance to achieve the final value of the phase shift is, however, strongly different on different reflections, as marked by the arrows. It takes up to 20 oscillations at the specular spot position in the  $[\bar{1}10]$  azimuth, whereas the phase shift is completed typically during the first oscillation in all other cases. The very short transition distance observed at the inverted interface implies that the sampling depth of the oscillating part of the RHEED signal is less than the 0.28 nm

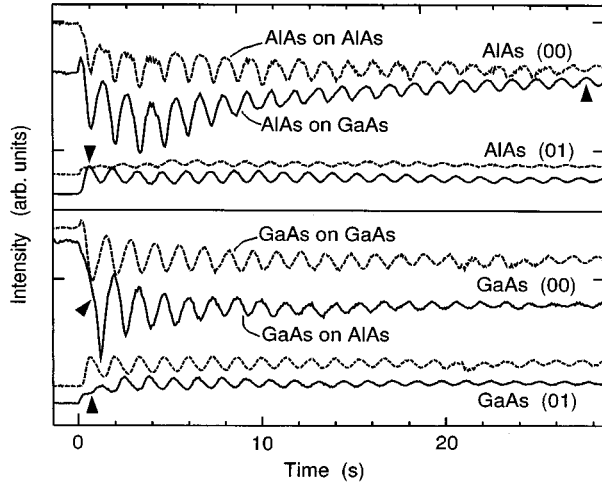


FIG. 1. Synchronized RHEED intensity oscillations from AlAs/GaAs and GaAs/AlAs interfaces recorded with an incidence angle of 0.35 degrees. For all 4 pairs of traces, the broken line is the homoepitaxial reference and the solid line represents the signal from heterointerface formation. The {01} intensities can only be measured outside the Laue circle at these low angles. The electron energy was 20 keV with the beam directed along the  $[\bar{1}10]$  azimuth. The growth rates were 0.2 nm/s at a sample temperature of 584 °C, and the  $\text{As}_4$  beam equivalent pressure was  $3.2 \times 10^{-3}$  Pa. The curves are shifted in the vertical direction for clarity.

(002) lattice plane spacing, denoted in the following as one bilayer. If it were larger, an abrupt interface gradually crossing the sampled volume would produce a gradually varying signal with a minimum transition distance equal to the probing depth. As we will show, the observed phase shift phenomena are closely connected to the surface reconstruction. We therefore call this class of effects the reconstruction-induced phase shifts (RIPS) of RHEED intensity oscillations.<sup>20</sup>

Diffraction-related shifts can be separated from growth-induced shifts by observing RHEED intensity oscillations at different diffraction conditions. A convenient way of doing this is the simultaneous recording at different positions of the RHEED pattern. This has already been done by the comparison of (00) and {01} streaks shown in Fig. 1. A second, more instructive way is the measurement setup indicated in Fig. 2. A line is placed along the (00) streak containing the specular spot, and the intensities along this line are subsequently recorded as a function of time. For the different positions along the streak, we again compare the heteroepitaxial traces to homoepitaxy. With a pulse sequence as in Fig. 1 and subsequent synchronization of the data, the line pairs in Fig. 3 are obtained. The oscillations from the AlAs-on-GaAs interface are shown as solid lines, the broken curves again representing homoepitaxial AlAs growth. All four pairs of traces end up with the same phase shift of  $\pi$ . However, the absolute phase positions of the solid or the broken curves differ by as much as half a period. Moreover, even the relative phase offset at the beginning of heterointerface formation is different within the different pairs. Whereas it is roughly in-phase for positions 1, 3, and 4, it is approximately out-of-phase for position 2. All signals originate from the same growing surface and are recorded simultaneously.

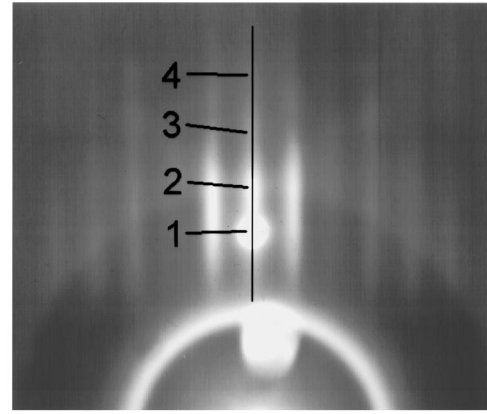


FIG. 2. Recording line position for the measurement shown in Fig. 3. The sample temperature was 547 °C at an  $\text{As}_4$  beam equivalent pressure of  $3.1 \times 10^{-3}$  Pa. The beam incidence angle was  $0.77^\circ$  using 20-keV electrons. The azimuth was  $[\bar{1}10]$ .

Different experiments with different incidence angles and azimuths reproduce this behavior. Whereas the absolute phase of the oscillations as well as the relative offset at the beginning of growth assume different values, the saturation value of the shift is the same, independent of diffraction conditions. This constitutes strong evidence that the final value of the phase shift is not diffraction induced, but related to the surface structure. Moreover, the data show that for the investigated surface there is no direct correspondence between surface step density and the oscillating RHEED intensity, since for the same growing surface, any phase can be observed with a suitable choice of diffraction conditions. Instead, the phase dispersion of RHEED intensity oscillations can be modeled by a layer refraction model that does not explicitly contain the step density.<sup>21,19</sup> This mechanism can also account for shifts in the absolute phase position as a function of  $\text{As}_4$  overpressure observed earlier.<sup>22,23</sup>

By additionally varying the growth conditions such as  $\text{As}_4$  pressure, sample temperature, and growth rates in simi-

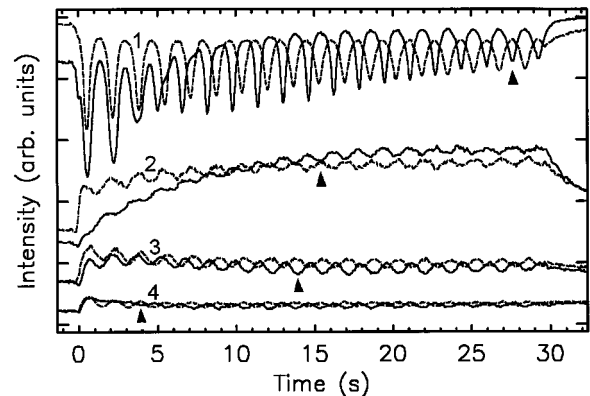


FIG. 3. Comparison of RHEED intensities for the different positions along the streak marked in Fig. 2. Similar to the difference between specular spot and (01) streak, the saturation distance of the RIPS decreases with distance from the specular spot. This indicates a disorder sensitivity on the specular spot compared to other locations in the diffraction diagram.

lar experiments, we conclude that the saturation value of the RIPS depends only on the two surface reconstructions before and after interface formation. Far from the interface, both traces monitor growth of AIAs on AIAs or GaAs on GaAs. The amplitudes of both curves in a pair are similar, indicating a similar surface morphology. Yet we obtain a constant phase shift. This means that there is a memory effect of the interface, as if material were lost or added during its formation. We therefore conclude that the RIPS saturation value cannot be a diffraction phenomenon. Instead, we link it to the difference in the group III element content of the two surface reconstructions. Since the growth is performed under  $As_4$  overpressure, the formation of a certain surface reconstruction is not constrained by the  $As_4$  supply. Instead, the constant group III flux during deposition defines the time axis of the RHEED oscillations. For homoepitaxy, the deposition of group III elements equal to the group III content of  $n$  bulk bilayers advances the growth front by  $n$  bilayers. However, the reconstructed layers at the surface may contain incomplete group III sublattices. If the reconstruction changes at the heterointerface, group III material is consumed or released during the transition, resulting in a shift of the remaining oscillations. Interpreting the phase shift in this way, we identify it with the loss or gain of the group III elements between the two surface reconstructions. This conclusion imposes constraints on different pairs of possible structure models for both surfaces. In our case, GaAs exhibits the  $\beta(2 \times 4)$  RHEED pattern using the Farrell-Palmström terminology<sup>24</sup> and AIAs shows the  $c(4 \times 4)$  pattern. From the phase shift we therefore conclude that the surface structures producing these patterns differ by half a (002) bilayer of Ga or Al. The most commonly discussed structure models for the  $\beta(2 \times 4)$  RHEED pattern as well as the  $c(4 \times 4)$  structure are well documented, see, e.g., Ref. 25. The most likely  $\beta(2 \times 4)$  structure exhibits a  $3/4$  top Ga layer layer coverage. The  $c(4 \times 4)$  (Ref. 26) structure has been investigated for GaAs. There are indications for a  $1/4$  to  $1/2$  top Ga layer coverage in this structure,<sup>27,28</sup> which would be consistent with electron counting arguments. If the AIAs  $c(4 \times 4)$  structure is similar to the GaAs  $c(4 \times 4)$ , the obtained  $1/2$  period shift would predict a  $1/4$  Al layer coverage, if we start from  $3/4$  Ga layers on the GaAs surface.

The phase shift between GaAs and AIAs implies a chemical sensitivity of the oscillation phase that should allow us to determine the surface composition during growth. We therefore replaced AIAs in our pulse sequence by  $Al_xGa_{1-x}As$  with varying  $x$  and obtained the curves shown in Fig. 4. The inverted interface was chosen because the rapid phase shift there increases the measurement accuracy. As will be shown later, the RIPS is independent of the growth rate in the range used. Therefore, the growth rates were optimized to obtain similar fluxes and growth dynamics for the  $Al_xGa_{1-x}As$  growth intervals being probed by the GaAs growth intervals shown. As in Fig. 1, the broken lines represent the homoepitaxial reference oscillations. Diffraction conditions were adjusted so that the initial phase shift at the beginning of the normal heterointerface formation was zero. The phase shift for both the specular spot and the (01) streak is the same. It relates to the surface composition as plotted in the lower part of the figure. This dependence identifies a given value of the oscillation phase with a certain nominal bulk composition.

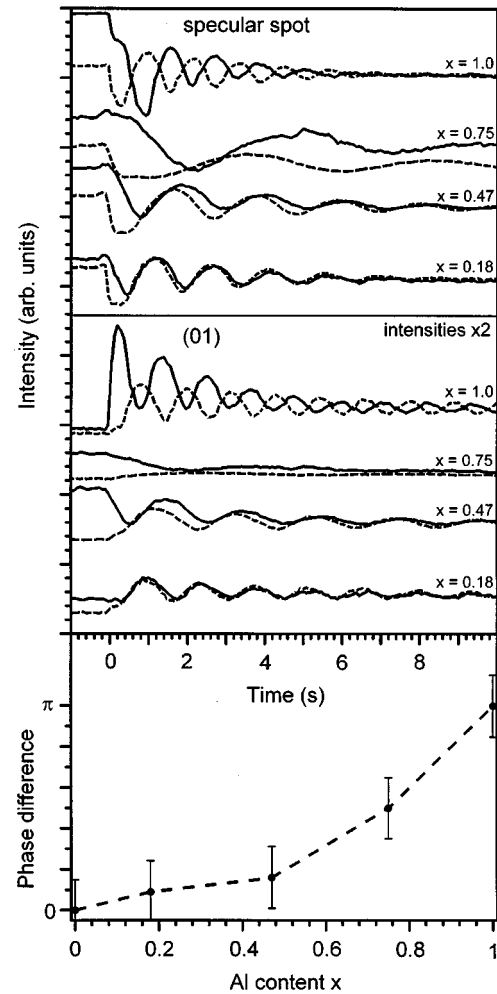


FIG. 4. Relationship between alloy composition  $x$  and phase shift. The AIAs was replaced by  $Al_xGa_{1-x}As$  in measurements using growth conditions similar to Fig. 1. The resulting dependence is plotted in the lower part of the figure. Shown are the curves for GaAs on GaAs (broken lines) and GaAs on  $Al_xGa_{1-x}As$  (solid lines) at the inverted interface. Both specular spot and first-order spot recorded in the same run produce the same phase shifts.

The surface composition can be different due to segregation. The similar phase shift on both the specular and first-order diffracted spots, however, suggests that segregation is small for the codeposition of both Ga and Al. The possible error is accounted for by the error bars in the plot.

From the specular spot signal obtained at the normal interface along  $[\bar{1}10]$ , we thus deduce strong segregation at the normal interface. The shift on the  $\{01\}$  streaks of the same measurement, however, is instantaneous, indicating no segregation. The surface material composition as a function of the deposited AIAs bilayers is plotted in Fig. 5 for both reflections. The profiles were calculated from the same measurement sequence as the calibration of Fig. 4.

The apparent contradiction between the specular spot and the (01) profiles is resolved by taking into account the morphology of the GaAs surface and the special scattering geometry of RHEED. Because of the small probing depth of the RHEED electrons, a deviation from the perfect translational symmetry of the top surface layer breaks the lateral

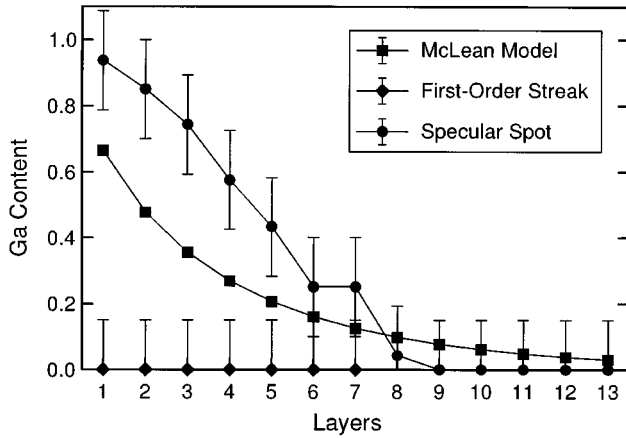


FIG. 5. Surface alloy composition determined with the relation of Fig. 4 at the specular spot position, the first-order diffraction streak and the theoretical curve using the McLean model with the parameters of Ref. 35.

symmetry of the surface for RHEED. Information from disordered surface regions is therefore detected at or near the specular spot, which would be the only peak in the diffraction pattern of a perfectly random two-dimensional (2D) structure containing all spatial frequencies. Ordered regions with complete lateral symmetry can contribute to all scattering orders. At the same time, the difference in phase shift saturation between the specular and the (00) spots is not present along the  $[110]$  azimuth, while its final value remains the same.<sup>29</sup> This indicates an anisotropy of the surface. The GaAs(001) surface in the  $\beta(2 \times 4)$  reconstruction exhibits an anisotropic morphology,<sup>30,31</sup> leading to long and relatively straight step edges along  $[\bar{1}10]$ . The most likely candidate for a symmetry-breaking surface defect therefore is a bilayer step. If the RHEED beam is parallel to the edges, it can sensitively accumulate the step edge signal, leading to a large variation in the specular spot oscillations. Perpendicular to the step edges, this accumulation is not present, and the RIPS saturates immediately.

This real-space sensitivity of RHEED leads us to conclude that segregation is a predominantly step-mediated process that is suppressed on the flat surface regions. The different binding energies of terrace and step atoms facilitate exchange reactions at steps. During layer-by-layer growth (2D nucleation), which corresponds to the case of weakly damped RHEED oscillations, a step present on the surface prior to growth propagates in the growth direction, being at roughly the same lateral position after the deposition of a complete bilayer.<sup>32</sup> During growth, it serves as a source of exchange reactions in the segregation process. Details are discussed below. The smaller scale islands causing the oscillations during deposition nucleate on the terraces where no Ga atoms are released from the complete underlying plane, and therefore no segregation is observed in higher diffraction orders.

Current RHEED theory does not yet allow the treatment of realistic stepped surfaces.<sup>33</sup> We therefore cannot determine the quantitative fraction of the segregating and nonsegregating regions on the surface directly from the diffraction pattern. Repetition of the RIPS experiment along the  $[110]$

azimuth<sup>29</sup> shows an immediately saturating shift on both streaks within the measurement accuracy, indicating that the fraction of segregation areas is small. A laterally homogeneous segregation profile is modeled for the GaAs-AIAs material system using McLean's formula<sup>34</sup>

$$\ln\left(\frac{x_b}{1-x_b}\right) = \frac{E_s}{kT} + \ln\left(\frac{x_s}{1-x_s}\right),$$

where  $x_s$  and  $x_b$  denote the surface and bulk compositions,  $E_s$  the difference between bulk and surface free energy, and thermal equilibrium between the surface bilayer and bulk material is assumed. Using parameters deduced from the fitting of electron spectroscopy experiments,<sup>35</sup> the curve plotted in Fig. 5 is obtained. Material exchange is only considered between the top bilayer and the bilayer immediately below. The RIPS values of the specular spot indicate a nonexponential segregation that would produce an approximately constant (top hat) concentration profile if it were homogeneous across the surface. The signal from the first-order spot indicates no segregation. These three results are consistent if the lateral extent of the intermixed region near the step diminishes during overgrowth, while the material composition at the step itself remains Ga rich with an almost constant composition. We therefore expect to obtain segregation in elongated regions that follow the surface steps.

To confirm our conclusion derived in the preceding paragraph, HRTEM micrographs shown in Fig. 6 were taken along the extremal directions of the surface anisotropy. Along  $[\bar{1}10]$ , laterally separated segregation regions are visible at the normal interface. Since the sample thickness corresponds to roughly 80  $\{110\}$  crystal planes, this finding implies a high degree of order along the beam direction, in agreement with the highly anisotropic surface morphology of GaAs. In the perpendicular  $[110]$  direction, the segregation regions are projected along their narrow direction, leading to a broad, featureless band. No segregation, as expected from the RHEED experiments, is seen at the normal heterointerface. The transition regions are marked by grey bars to the side. The small lateral separation of the segregation regions might be due to kinks in the step edge that typically shift the step by four lattice constants, the periodicity of the  $\beta(2 \times 4)$  reconstruction in this direction.

The assumption of a thermal equilibrium in the McLean model requires that this equilibrium is approached faster than the typical time scales involved in the growth process. We have investigated the kinetics of the segregation by varying the AIAs growth rate in experiments otherwise similar to the one shown in Fig. 1. The measured transition distances of the phase shift are shown in Fig. 7, marked by the solid arrows. The growth and diffraction conditions were otherwise identical for the three curves. Open arrows indicate the transition distance of the 1.27 Å/s curve. The larger transition distance at higher growth rates indicates that the exchange process is not kinetically limited. Instead, we can conclude that segregation takes place in a local equilibrium situation. As well, the saturation value of the RIPS far from the heterointerface is not affected by the different growth kinetics, again confirming our assumption that it does not depend on surface roughness or the morphological evolution of the growth front.

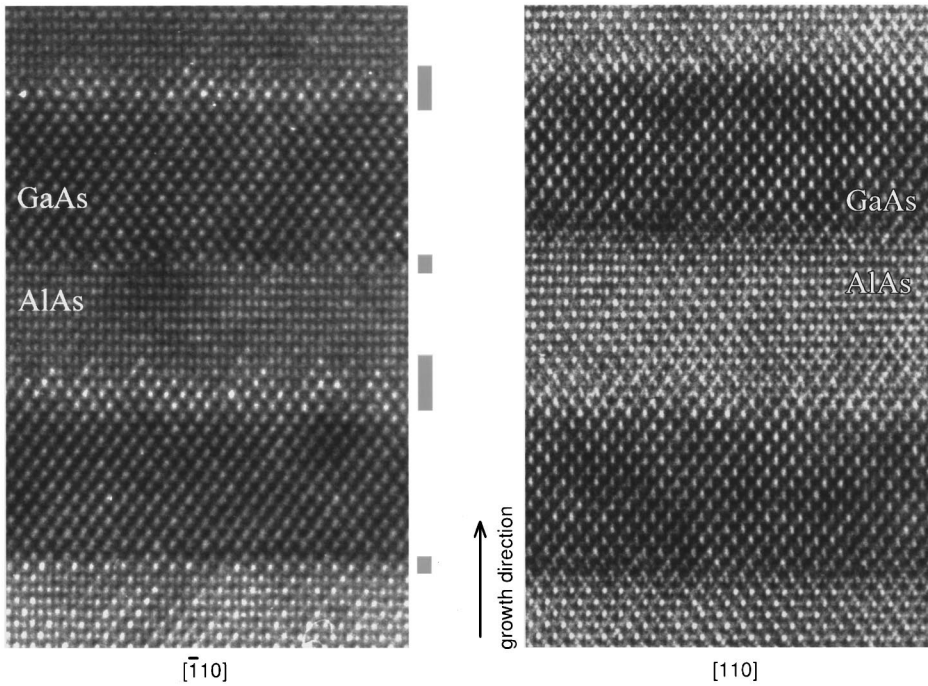


FIG. 6. HRTEM micrographs along two azimuths of a nominal 14 bilayer/14 bilayer GaAs/AlAs superlattice. The growth conditions for the sample were similar to those detailed in Fig. 1. The electron energy was 400 keV.

Similar data taken as a function of temperature are shown in Fig. 8. Due to the large transition distances of the RIPS and the noise on the data, a reliable determination of the distances is difficult. An Arrhenius fit to the solid arrows, marked by the open ones, yields an activation energy of 0.5 eV and the presence of a kinetical barrier for the process, since the McLean model would predict a decrease of the segregation length with temperature.

The inconsistent behavior of the two measurements indicates the limited validity of a simple one-dimensional model to describe the segregation process. Instead, processes both parallel and perpendicular to the surface have to be taken into account. This is shown for our hypothesis of a step-

mediated process in Fig. 9. In this simple atomistic picture, GaAs units are represented by hatched areas, AlAs units by open squares. For the two initial states of an AlAs unit approaching the step from below or above, the four final states directly after interaction with the step are shown in (a)–(d). Processes (a) and (b) represent the attachment to the step, including a change of the level for (a) with approach from the left or (b) with approach from the right. Processes (c) and (d) additionally involve the exchange of GaAs and AlAs

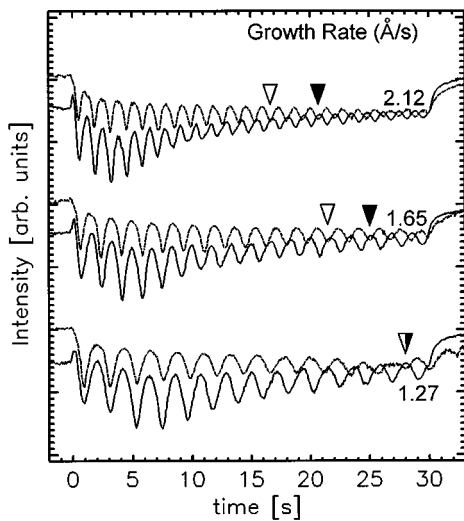


FIG. 7. Variation of the RIPS saturation distance as a function of the growth rate. The values determined from the graph are marked by solid arrows, while the low growth rate distance is indicated by open arrows.

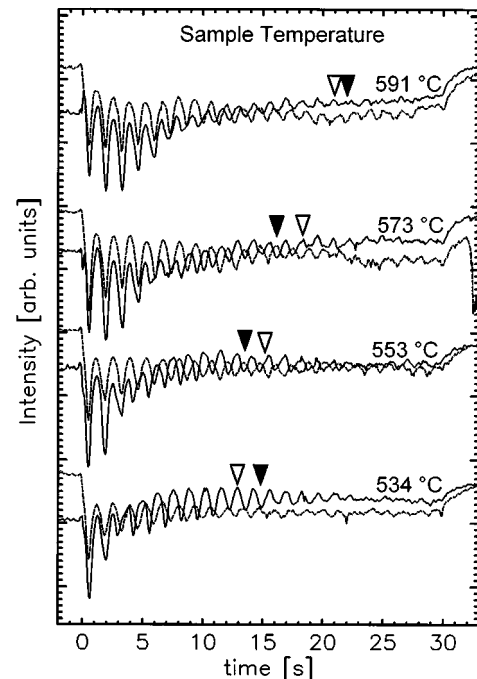


FIG. 8. Variation of the RIPS saturation distance with sample temperature. The solid arrows indicate the measured values, open arrows show an Arrhenius fit.

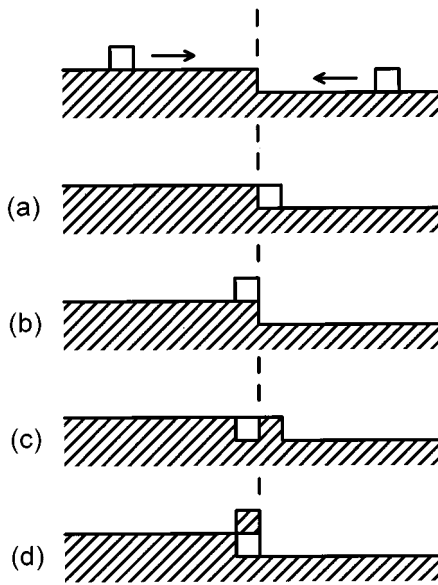


FIG. 9. Atomistic model for segregation at a heteroepitaxial step edge. GaAs units are denoted by hatched areas, AlAs units by open squares. For a GaAs unit approaching from the lower or upper level, any of the four final states (a)–(d) is possible, resulting in eight different events.

units. This results in eight possibilities, four of which [(c) and (d)] lead to alloy formation at the step. A rate equation model using these eight processes would involve eight transition probabilities, all of which are in principle unknown. Therefore, even a good fit to the experimental data would probably be of limited value. However, we can immediately conclude that for a step-mediated segregation mechanism at the heterointerface, at least processes (d) must have a significant probability, since they are the ones providing GaAs material transport to the upper layer. Processes (c) are responsible for lateral alloy formation. Both (c) and (d) must be

present to obtain the triangularly shaped segregation features observed in Fig. 6. Note that both processes (c) and (d) imply that the *center of the alloy* either moves slightly left or is stationary, in contrast to the *morphological step edge* position, which moves right with (a) or (c). For equal deposition rates on the lower and upper terraces, the movement of the morphological step position depends on the net difference between the processes that move a unit up and down the step, respectively. This indicates that a step-mediated segregation process is able to produce the features observed in the Fig. 6 TEM cross sections, namely, laterally symmetric and well-aligned features, even if the morphological step edge is moving due to a predominant step-down process. Instead, the important requirement is that the lateral center of the alloyed region remains stationary.

#### IV. CONCLUSION

We have shown that the difference of the reconstruction-induced phase shifts of RHEED oscillations at specular and nonspecular positions can be explained by the morphological sensitivity of RHEED. We discovered strong laterally anisotropic Ga segregation for MBE growth of AlAs on GaAs(001), whereas no segregation is found for deposition of GaAs on AlAs(001). The RIPS measurement method is nondestructive, *in situ* and allows data acquisition in real time during the formation of the interface. It relies only on the surface reconstruction difference, the presence of RHEED intensity oscillations, and the requirement that only one of the deposition fluxes is rate limiting. It should therefore be applicable to any materials system that meets these requirements.

#### ACKNOWLEDGMENTS

The authors gratefully acknowledge the support of the Deutsche Forschungsgemeinschaft (Sonderforschungsbereich 296) and thank Oliver Brandt for helpful discussions.

\*Electronic address: braun@pdi.wias-berlin.de, www:http://pdil.wias-berlin.de/~braun

<sup>1</sup>J. F. Zheng, J. D. Walker, M. B. Salmeron, and E. R. Weber, *Phys. Rev. Lett.* **72**, 2414 (1994).

<sup>2</sup>H. Yamaguchi and Y. Horikoshi, *J. Appl. Phys.* **68**, 1610 (1990).

<sup>3</sup>E. Molinari, S. Baroni, P. Gianozzi, and S. de Gironcoli, *Phys. Rev. B* **45**, 4280 (1992).

<sup>4</sup>S. M. Hu, D. C. Ahlgren, P. A. Ronsheim, and J. O. Chu, *Phys. Rev. Lett.* **67**, 1450 (1991).

<sup>5</sup>S. Fukatsu, K. Fujita, H. Yaguchi, Y. Shiraki, and R. Ito, *Appl. Phys. Lett.* **59**, 2103 (1991).

<sup>6</sup>D. E. Jesson, S. J. Pennycook, J.-M. Baribeau, and D. C. Houghton, *Phys. Rev. Lett.* **68**, 2062 (1992).

<sup>7</sup>G. S. Spencer, J. Menéndez, L. N. Pfeiffer, and K. W. West, *Phys. Rev. B* **52**, 8205 (1995).

<sup>8</sup>B. Etienne and F. Laruelle, *J. Cryst. Growth* **127**, 1056 (1993).

<sup>9</sup>B. Jusserand and F. Mollot, *Appl. Phys. Lett.* **61**, 423 (1992).

<sup>10</sup>P. M. Young and H. Ehrenreich, *Appl. Phys. Lett.* **61**, 1069 (1992).

<sup>11</sup>J. Massies, F. Turco, A. Saletes, and J. P. Contour, *J. Cryst. Growth* **80**, 307 (1987).

<sup>12</sup>V. Thierry-Mieg, F. Laruelle, and B. Etienne, *J. Cryst. Growth* **127**, 1022 (1993).

<sup>13</sup>O. Dehaese, X. Wallart, and F. Mollot, *Appl. Phys. Lett.* **66**, 52 (1995).

<sup>14</sup>J. F. Nützel and G. Abstreiter, *Phys. Rev. B* **53**, 13 551 (1996), and references therein.

<sup>15</sup>B. L. Olmsted and S. N. Houde-Walter, *Appl. Phys. Lett.* **63**, 530 (1993).

<sup>16</sup>J. Zhang, J. H. Neave, P. J. Dobson, and B. A. Joyce, *Appl. Phys. A* **42**, 317 (1987).

<sup>17</sup>W. Braun, L. Däweritz and K. H. Ploog (unpublished).

<sup>18</sup>W. Braun and K. Ploog, *Appl. Phys. A* **60**, 441 (1995).

<sup>19</sup>Y. Horio and A. Ichimiya, *Surf. Sci.* **298**, 261 (1993).

<sup>20</sup>F. Briones, D. Golmayo, L. Gonzalez, and J. L. De Miguel, *Jpn. J. Appl. Phys.* **24**, L478 (1985).

- <sup>23</sup>W. Braun, Ph. D. thesis (Berlin, 1996).
- <sup>24</sup>H. H. Farrell and C. J. Palmström, *J. Vac. Sci. Technol. B* **8**, 903 (1990).
- <sup>25</sup>For a recent discussion, see T. Hashizume, Q.-K. Xue, A. Ichimiya, and T. Sakurai, *Phys. Rev. B* **51**, 4200 (1995), and references therein.
- <sup>26</sup>D. K. Biegelsen, R. D. Bringans, J. E. Northrup, L.-E. Swartz, *Phys. Rev. B* **41**, 5701 (1990).
- <sup>27</sup>J. Falta, R. M. Tromp, M. Copel, G. G. Pettit, P. D. Kirchner, *Phys. Rev. Lett.* **69**, 3068 (1992).
- <sup>28</sup>H. Nörenberg and N. Koguchi, *Surf. Sci.* **296**, 199 (1993).
- <sup>29</sup>W. Braun and K. H. Ploog, *J. Appl. Phys.* **75**, 1993 (1994).
- <sup>30</sup>E. J. Heller and M. G. Lagally, *Appl. Phys. Lett.* **60**, 2675 (1992).
- <sup>31</sup>J. Sudijono, M. D. Johnson, M. B. Elowitz, C. W. Snyder, B. G. Orr, *Surf. Sci.* **280**, 247 (1993).
- <sup>32</sup>B. A. Joyce, N. Ohtani, S. M. Mokler, T. Shitara, J. Zhang, J. H. Neave, and P. N. Fawcett, *Surf. Sci.* **298**, 399 (1993).
- <sup>33</sup>For some recent work on the GaAs(001) surface, see Y. Ma, S. Lordi, P. K. Larsen, J. A. Eades, *Surf. Sci.* **289**, 47 (1993); J. M. McCoy, U. Korte, P. A. Maksym, G. Meyer-Ehmsen, *Phys. Rev. B* **48**, 4721 (1993).
- <sup>34</sup>D. McLean, *Grain Boundaries in Metals* (Oxford University Press, Oxford, 1957), p. 116ff.
- <sup>35</sup>J. M. Moison, C. Guille, F. Houzay, F. Barthe, and M. Van Rompay, *Phys. Rev. B* **40**, 6149 (1989).